Article

Performance Investigation of a Two-Bed Type Adsorption Chiller with Various Adsorbents

Jung-Gil Lee, Kyung Jin Bae and Oh Kyung Kwon *

Thermal and Fluid System Group, Korea Institute of Industrial Technology, Cheonan-si, Chungcheongnam-do 31056, Korea; jglee@kitech.re.kr (J.-G.L.); kjbae@kitech.re.kr (K.J.B.)
* Correspondence: kwonok@kitech.re.kr; Tel.: +82-041-589-8528

check for updates

Abstract: In this study, the performance evaluation of an adsorption chiller (AD) system with three different adsorbents—silica-gel, aluminum fumarate, and FAM-Z01—was conducted to investigate the effects of adsorption isotherms and physical properties on the system's performance. In addition, the performance evaluation of the AD system for a low inlet hot-water temperature of 60 °C was performed to estimate the performance of the system when operated by low quality waste heat or sustainable energy sources. For the simulation work, a two-bed type AD system is considered, and silica-gel, metal organic frameworks (MOFs), and ferro-aluminophosphate (FAPO, FAM-Z01) were employed as adsorbents. The simulation results were well matched with the laboratory-scale experimental results and the maximum coefficient of performance (COP) difference was 7%. The cooling capacity and COP of the AD system were investigated at different operating conditions to discuss the influences of the adsorbents on the system performance. Through this study, the excellence of the adsorbent, which has an S-shaped isotherm graph, was presented. In addition, the influences of the physical properties of the adsorbent were also discussed with reference to the system performance. Among the three different adsorbents employed in the AD system, the FAM-Z01 shows the best performance at inlet hot water temperature of 60 °C, which can be obtained from waste heat or sustainable energy, where the cooling capacity and COP were 5.13 kW and 0.47, respectively.

Keywords: adsorption chiller; adsorbent; isotherm characteristics; coefficient of performance; cooling capacity; simulation; metal organic frameworks; low quality waste heat; sustainable energy

1. Introduction

As the quality of life improves, the cooling demands in residential and industrial sites are increasing. The ambient temperature affects the quality of human life and human health. Generally, compressor-based cooling processes are adopted to cool down indoor spaces such as residences, work places, and factories due to their convenience of use. Although equipment for compressor-based cooling processes generally occupies a relatively small space, it is high in energy consumption. The high demand for electricity may cause blackouts during the summer season, and also accelerate global warming due to its high dependence on fossil fuels. Therefore, the development of alternative cooling technologies that can replace compressor-based cooling processes is necessary for the mitigation of global warming, air pollution, and excessive electrical energy consumption.

This work discusses an eco-friendly and sustainable adsorption chiller (AD) which does not use ozone depletion gases and has low energy requirements. The AD system operates based on the adsorption and desorption processes by the porous adsorbent. The isotherm characteristics and physical properties of the adsorbent influence the system's performance. Silica-gel is generally employed as an adsorption agent in AD systems, as it is cheap [1]. The adsorption and desorption rates of silica-gel increase linearly with the relative pressure. The linear isotherm characteristics of

silica-gel are predictable and can control the system performance according to the operating conditions; however, its desorption process requires relatively high hot-water temperature, around 80 °C [2].

Therefore, the development of the novel adsorbent in terms of the structure, materials, etc., has been undertaken to enhance the system's performance. To enhance the system performance, the novel adsorbent has to have the following characteristics: (i) high adsorption and desorption rates under the operating conditions, (ii) high pre-exponential constant of surface diffusivity, (iii) high specific surface area, and (iv) low adsorption heat.

Extensive research has been conducted on the performance evaluation of an AD system with silica-gel as an adsorbent [2–14]. Those studies aimed to evaluate system performance with various operating conditions experimentally or numerically and to optimize the system performance. Saha et al. [2] presented a numerical analysis for the performance evaluation of a silica-gel water AD system to estimate the influences of operating conditions on AD system performance. In addition, various adsorbents were developed as adsorption agents in the AD system to enhance the system performance [15–26]. The performance evaluation studies of the AD system were conducted with FAM-Z01, which is manufactured based on zeolite material [15–18]. The FAM-Z01 has an S-shape isotherm graph, and the adsorption and desorption rates may exhibit sudden jumps at certain relative pressure values. Therefore, the AD system with FAM-Z01, which has S-shape isotherm characteristics, can utilize a lower hot-water temperature for the desorption process. Hong et al. [17] and Kim et al. [18] showed the system performance of the AD system with FAM-Z01 and demonstrated the excellent effect of the S-shape isotherm characteristics on the system performance. In addition, a new class of metal organic framework (MOF) adsorbents was developed, which have been projected as next-generation adsorbents due to their advantages such as high surface area, high degree of porosity, and possible fine-tuning of chemical structure [19–26].

Although previous studies discussed the advantages of S-shaped isotherms, they did not compare the performances of the adsorbents which have S-shape isotherm characteristics. In this study, therefore, by comparing silica-gel, aluminum fumarate, and FAM-Z01, the influences of the physical properties and isotherm characteristics of the adsorbent on the system performance were discussed, numerically. The two-bed type AD system was adopted to investigate the influence of the adsorbent on the AD system's performance and a numerical analysis was conducted. The two-bed type AD system has two beds which each have an adsorbent coated heat exchanger. Therefore, the two-bed type AD system can proceed with the adsorption mode and desorption mode simultaneously at each bed. The performance evaluation of the AD system was conducted at the lower inlet hot water temperature which can be achieved by using low-quality waste heat or sustainable energy heat sources, such as solar and geothermal energy. The influence of the adsorbent on the system performance was compared and discussed under various operating conditions.

2. Materials and Methods

2.1. Experimental Set-Up

In order to validate the numerical model, a laboratory-scale experimental study has been conducted for the two-bed type AD system with FAM-Z01. A picture of real equipment can be seen in Figure 1 and the experimental set-up consisted of two beds for adsorption and desorption processes, a condenser, an evaporator, a data acquisition system, circulation pumps, a vacuum pump, a boiler and a chiller, and control valves. The pressure and temperature of the adsorption and desorption beds and evaporator were measured by a vacuum pressure gauge (range: 0–13.3 kPa, error: ±0.25% reading) and a resistance temperature detector (RTD, range: −200–400 °C, error: ±0.01 °C), respectively. The FAM-Z01 was coated on the copper plate surface of heat exchanger. The operating conditions of experimental study can be seen in Table 1.
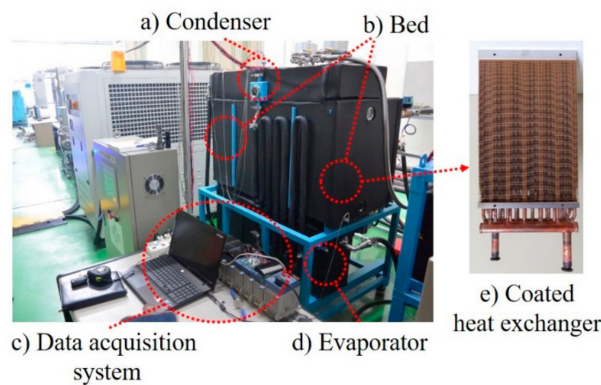
Figure 1. Picture of an adsorption chiller (AD) system.

Table 1. Operating conditions of laboratory-scale test.

Weight of Adsorbent (kg)	Chilled Water Temp. (°C)	Cooling Water Temp. (°C)	Hot Water Temp. (°C)	Cooling Water Flow Rate (kg/s)	Hot Water Flow Rate (kg/s)	Chilled Water Flow Rate (kg/s)	Cycle Time (sec)	Fixed U·A Adsorber/ Condenser/ Evaporator (W/K)
8 (each bed)	13	27–33	80	1.0	1.0	0.7	420	1430/4500/ 1170

*U: overall heat transfer coefficient, and A: area.

To calculate the cooling capacity and heat load, the inlet and outlet chilled water temperatures and inlet and outlet hot water temperature were measured by the each RTD sensor every one second, respectively. The cooling capacity and heat load were calculated by the difference between the inlet and outlet chilled water temperatures and difference between the inlet and outlet hot water temperatures. The coefficient of performance (COP), cooling capacity, and heat load were calculated with Equations (1)–(3).

$$COP = Q_{Chilled} / Q_{hot} \tag{1}$$

$$Cooling\ capacity(Q_{Chilled}) = m_{chilled} \cdot C_{P,chilled} \cdot (T_{in,chilled} - T_{out,chiilled}) \tag{2}$$

$$Heat\ load(Q_{hot}) = m_{hot} \cdot C_{p,hot} \cdot (T_{in,hot} - T_{out,hot}) \tag{3}$$

The error between the predicted results and experimental results was calculated with Equation (4).

$$Error(\%) = (COP_{Pre.} - COP_{Exp.}) \times 100 / COP_{Pre.} \tag{4}$$

2.2. Adsorbent

The adsorbents employed in the system are introduced briefly in this section based on the isotherm characteristics that depict the adsorption and desorption rate and physical properties. The adsorbent used in the AD system has a porous structure that can adsorb the water vapor. The adsorption and desorption processes show an exothermic reaction and an endothermic reaction, respectively. Owing to the physical adsorption/desorption, the characteristics of the adsorbent did not change during the process. The detailed physical properties of the adsorbents are shown in Table 2.

Table 2 presents the pre-exponential constant of surface diffusivity, activation energy of diffusion, and heat of adsorption for each of the three different adsorbents. The heat of adsorption for FAM-Z01 is slightly higher than those of the others. The activation energy of diffusion for aluminum fumarate was around one third of the values of the others. The pre-exponential constant of surface diffusivity and particle size of aluminum fumarate were significantly lower than those of the others, indicating

that it has a larger effective surface area. The weight of each of the three different adsorbents used in the simulation studies was 47 kg.

Table 2. Physical properties of adsorbents.

Property	Silica-Gel [2]	Aluminum Fumarate [22,27,28]	FAM-Z01 [17]
Pre-exponential constant of surface diffusivity (D_{so}, m²/s)	2.54×10^{-4}	3.63×10^{-14}	2.54×10^{-4}
Activation energy of diffusion (E_a, J/mol)	45,500	18,026	42,000
Particle size (r, m)	0.2×10^{-3}	0.65×10^{-6}	0.2×10^{-3}
Specific heat (c_p, J/kg·K)	921	900	805
Heat of adsorption (Q_{st}, kJ/kg)	2430	2780	3109

Figure 2 shows the isotherm characteristics of the adsorbent for (a) silica-gel, (b) aluminum fumarate, and (c) FAM-Z01. The equations of isotherm graphs were well validated with the experimental data, and the current calculated values were well matched [2,18,22]. The silica-gel has a linear plot; i.e., the adsorption and desorption rates increase linearly with an increase in the pressure. Therefore, when silica-gel is employed as an adsorbent in the AD system, a higher hot-water temperature is required to enhance the desorption rate of the adsorbent. Meanwhile, the aluminum fumarate and FAM-Z01 has S-shaped isotherm characteristics. The main advantage of adsorbents which have S-shape isotherm characteristics is that they can have sudden changes in adsorption and desorption rates at the operating temperatures. In addition, the desorption process does not require a higher hot-water temperature than that of silica-gel. That is, the AD system with an adsorbent having an S-shaped isotherm can reduce the additional thermal energy requirement for increasing the hot water temperature. It means that the time and energy for achieving steady state of adsorption or desorption can be mitigated compared with the adsorbents which have linear isotherm characteristics. The advantage of the S-shaped isotherm characteristic is that the desorption process does not require a higher hot-water temperature than that of silica-gel. That is, the AD system with an adsorbent having an S-shaped isotherm can reduce the additional thermal energy requirement for increasing the hot water temperature.

Between two different adsorbents which have S-shape isotherm characteristics, the adsorption rate of aluminum fumarate is around two times higher that of FAM-Z01. Moreover, among the three different adsorbents, aluminum fumarate has the highest adsorption rate at low pressure. In addition, two adsorbents showed differences in physical properties, such as pre-exponential constant of surface diffusivity, activation energy of diffusion, particle size, specific heat, and heat of adsorption. The one of motivations for this study was to reveal the influences of the physical properties and adsorption and desorption rates of the adsorbent on the system performance.

2.3. Theoretical Approaches

Figure 3 shows the schematic diagram of an AD system. The V.P, C.P, and FCU in Figure 3 mean vacuum pump, circulation pump, and fan coil unit, respectively. The simulation featured a two-bed type AD system, and the heat and mass recovery schemes were not considered. In this section, the equations of the isotherm characteristics of the adsorbent, the adsorption and desorption rate, and the heat and mass balance are briefly introduced. A major assumption of this simulation study is that the effect of the non-condensable gas can be neglected. The adsorption equilibriums based on the saturation pressure for silica-gel, aluminum fumarate, and FAM-Z01 can be shown in Equations (5)–(7), respectively [2,18,22]. Those equations were well validated with the experimental data [2,18,22], and the estimated adsorption/desorption rate with respect to the pressure can be shown in Figure 2.
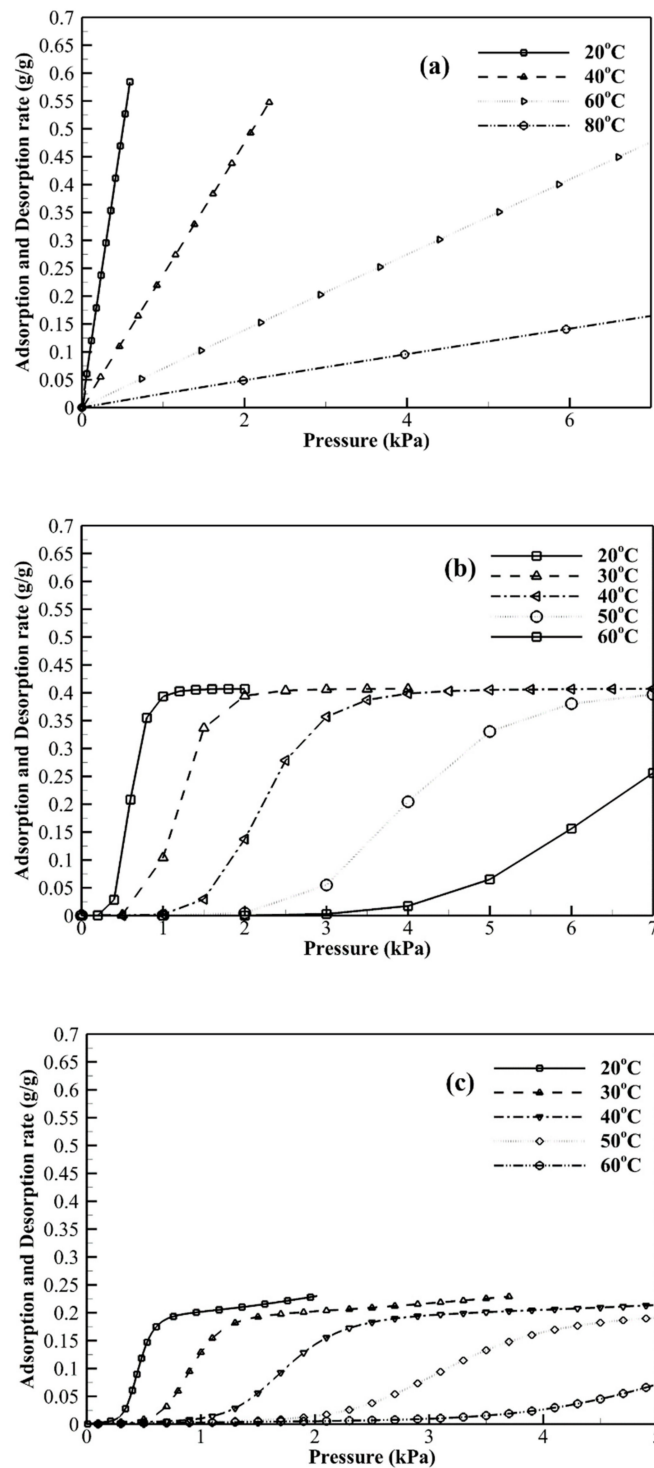
Figure 2. Isotherm characteristics of adsorbents according to the saturation pressure, such as: (**a**) silica-gel [2]; (**b**) aluminum fumarate [22], and (**c**) FAM-Z01 [18] at various temperatures.

$$q^* = A_0(T_S) \cdot [P_S(T_W)/P_S (T_S)]^{B(T_S)} \tag{5}$$

$$q^*/q^{\max} = K(P/P_S)^m / [1 + (K-1)(P/P_S)^m] \tag{6}$$

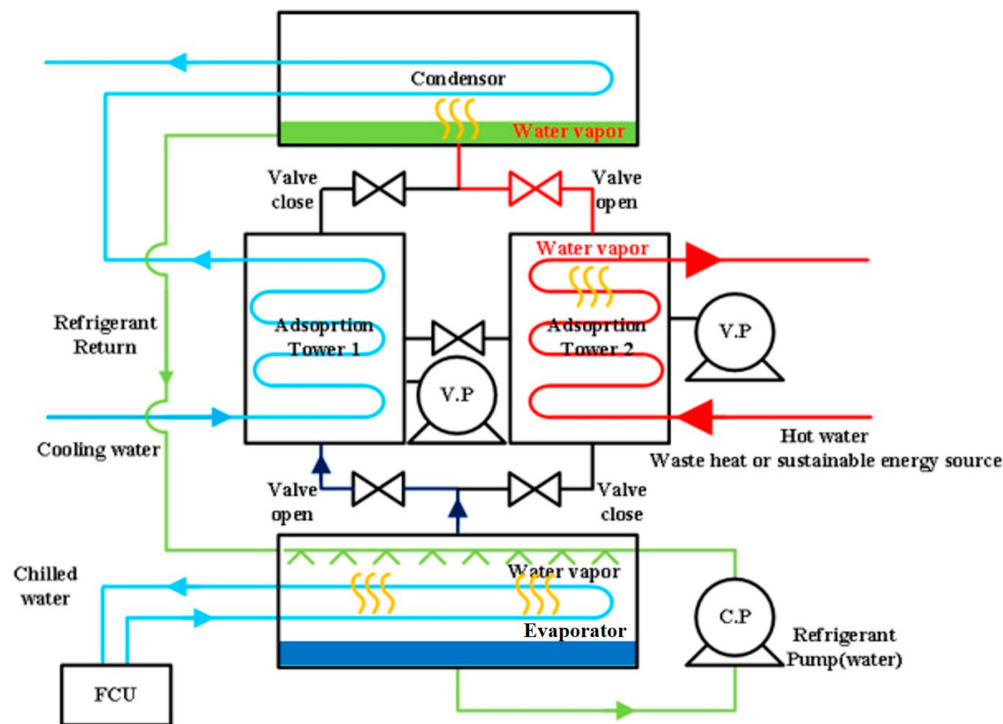$$q^* = \beta K_{Henry}(P/P_S) + (1-\beta)q^{\max}(K_{Sips}P/P_{Sips})^{1/n} / [1 + (K_S P/P_S)^{1/n}] \tag{7}$$

Figure 3. Schematic diagram of an AD system.

A fin-tube type heat exchanger was employed, and the materials of the fin and tube are copper and aluminum, respectively.

The Equations of the adsorption/desorption rate are as follows [2]:

$$D_S = D_{S0} \cdot \exp[-\frac{E_a}{RT_W}] \tag{8}$$

$$k_{sap} = 15\frac{D_S}{r_P^2} \tag{9}$$

$$\frac{dq}{dt} = k_{sap} \cdot (q^* - q) \tag{10}$$

The Equation of mass balance is expressed as follows:

$$\frac{dW_w}{dt} = W_{adsorbent} \cdot [-\frac{dq_{desorption}}{dt} + \frac{dq_{adsorption}}{dt}] \tag{11}$$

The Equations of (i) adsorption heat and energy balance, (ii) desorption heat and energy balance, (iii) evaporation heat and energy balance, (iv) condensation heat and energy balance, and (v) cooling capacity and coefficient of performance (COP) are as follows [2]:

(i) Adsorption heat and energy balance:

$$T_{out,CW} = T_{Adsorbent} + (T_{in,CW} - T_{Adsorbent}) \cdot \exp[-U_{Adsorbent}A_{HX}/m_{CW}c_{P,CW}] \tag{12}$$

$$\frac{d}{dt}((W_{Adsorbent} \cdot (C_{P,Adsorbent} + C_{P,CW} \cdot q_{Adsorption}) + (C_{P,Cu}W_{K,HX} + C_{P,Al} \cdot W_{F,HX})) \cdot T_{Adsorbent})$$
$$= Q_{st} \cdot W_{Adsorbent} \cdot \frac{dq_{Adsorption}}{dt} + m_{CW} \cdot C_{p,CW} \cdot (T_{in,CW} - T_{out,CW}) \tag{13}$$

(ii) Desorption heat and energy balance:

$$T_{out,HW} = T_{Desorbent} + (T_{in,HW} - T_{Desorbent}) \cdot \exp[-U_{Desorption}A_{HX}/m_{HW}c_{P,HW}] \tag{14}$$

$$\frac{d}{dt}\left(\left(W_{Adsorbent} \cdot (C_{P,Adsorbent} + C_{P,HW} \cdot q_{Desorption}) + (C_{P,Cu}W_{K,HX} + C_{P,Al} \cdot W_{F,HX})\right) \cdot T_{Desorbent}\right)$$
$$= Q_{st} \cdot W_{Adsorbent} \cdot \frac{dq_{Desorption}}{dt} + m_{HW} \cdot C_{p,HW} \cdot (T_{in,HW} - T_{out,HW}) \tag{15}$$

(iii) Evaporation heat and energy balance:

$$T_{out,Chilled} = T_{Eva} + (T_{in,Chilled} - T_{Eva}) \cdot \exp[-U_{Eva}A_{Eva}/m_{Chilled}c_{P,Chilled}] \tag{16}$$

$$\frac{d}{dt}\left((C_{P,Chilled} \cdot W_{EW} + C_{P,Cu} \cdot W_{Eva}) \cdot T_{Eva}\right)$$
$$= -L_W \cdot W_{Adsorbent} \cdot \frac{dq_{Adsorption}}{dt} + m_{Chilled} \cdot C_{P,Chilled} \cdot (T_{in,Chilled} - T_{out,Chilled}) \tag{17}$$
$$- C_{P,Chilled} \cdot T_{CW} \cdot W_{Adsorbent} \cdot \frac{dq_{Desorption}}{dt}$$

(iv) Condensation heat balance:

$$T_{out,CW} = T_{CW} + (T_{in,CW} - T_{CW}) \cdot \exp[-U_{CW}A_{CW}/m_{CW}c_{P,CW}] \tag{18}$$

$$C_{P,Cu} \cdot W_{CW} \cdot \frac{dT_{CW}}{dt} = -L_W \cdot W_{Adsorbent} \cdot \frac{dq_{Desorption}}{dt}$$
$$+ m_{CW} \cdot C_{P,CW} \cdot (T_{in,CW} - T_{out,CW}) \tag{19}$$
$$+ C_{P,CW} \cdot T_{CW} \cdot W_{adsorbent} \cdot \frac{dq_{Desorption}}{dt}$$

Figure 4 shows the solution procedure for the performance evaluation of the AD system. In this numerical model, the equations are solved sequentially while updating the parameters until the convergence criteria are satisfied. Intel Visual Fortran (USA, California) was employed as a simulation tool, and the solver employed in Intel Visual Fortran was the iteration method with convergence criteria (10^{-4}).

2.4. Operating Conditions

Table 3 shows the operating conditions of the two-bed type AD system employed in comparison study for performance investigation of three different adsorbents. Table 4 shows the control algorithm for the two-bed type AD system. The water vapor is filled in the pore of micro porous adsorbent by the van der Walls force during the adsorption process. The fully filled pore requires the desorption process to remove the water vapor from the pore to conduct the adsorption process, repeatedly. The pre-heating and pre-cooling modes are required to mitigate the performance degradation, which may occur under unsuitable operating conditions. The durations of the adsorption and desorption processes are 420 s, respectively, and the time taken for pre-heating or pre-cooling is 30 s. In summary, in the two-bed type AD system, the condenser and adsorption bed valves are opened for adsorption mode, and the adsorption bed and evaporator valves are opened, for 420 s, simultaneously. Then, the adsorption and desorption beds, evaporator, and condenser valves are all closed for 30 s for pre-heating and pre-cooling for the adsorption bed and desorption bed, respectively. Table 5 summarizes the physical properties of the two-bed type AD system adopted for performance evaluations of three different adsorbents, which were obtained from previous literature [2].

Table 3. Operating conditions of two-bed type AD system.

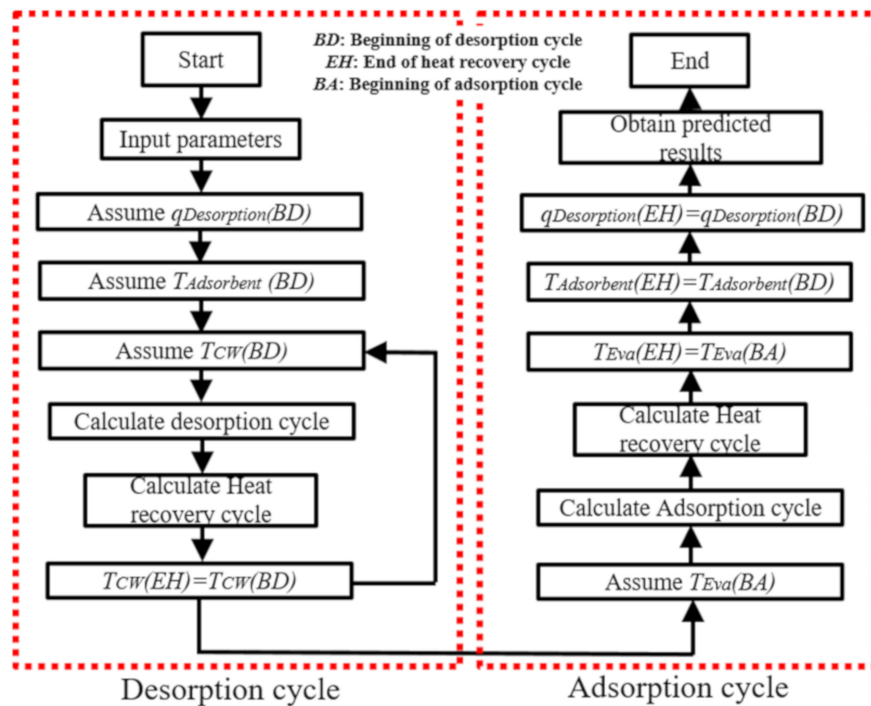| Weight of Adsorbent (kg)	Chilled Water Temp. (°C)	Cooling Water Temp. (°C)	Cooling Water Flow Rate (kg/s)	Hot Water Flow Rate (kg/s)	Chilled Water Flow Rate (kg/s)	Cycle Time (sec)	Fixed UA Adsorber/ Condenser/ Evaporator (W/K)
47	14	30	1.7	1.7	0.7	420	2460/11190/1910

Figure 4. Solution procedure.

Table 4. Control algorithm of the two-bed type AD system.

Cycle		Desorption	Pre-Heating Pre-Cooling	Adsorption	Pre-Heating Pre-Cooling
Time(s)		420	30	420	30
Valve	Adsorption	X	X	O	X
	Condenser	O	X	X	X
	Desorption	O	X	X	X
	Evaporator	X	X	O	X
Heat exchanger	Bed 1	Cold water	Hot water	Hot water	Cold water
	Bed 2	Hot water	Cold water	Cold water	Hot water

Table 5. Physical properties of two-bed type AD system [2].

Property	Value
A_{Cond} (m^2)	3.73
A_{Eva} (m^2)	1.91
A_{HX} (m^2)	2.46
$C_{P,Al}$ (J/kg·K)	905
$C_{P,Cu}$ (J/kg·K)	386
$C_{p,W}$ (J/kg·K)	4180
L_w (J/kg)	2.5×10^6
W_{Cond} (kg)	24.28
W_{Eva} (kg)	12.45
W_{EW} (kg)	50.00
$W_{F,HX}$ (kg)	64.04
$W_{K,HX}$ (kg)	51.20

3. Results

3.1. Model Validation

For model validation, a comparison study was conducted between the predicted results and experimental results. The experimental results were obtained from the two-bed type AD system with FAM-Z01. The comparison study of COP was conducted between the experimental results and predicted results at the given operating conditions, as shown in Table 1. The COP behavior obtained from the experiment and simulation is shown in Figure 5. The two results agree well within an error range of around 9.8%, which confirms the validation of the simulation model used in this research.
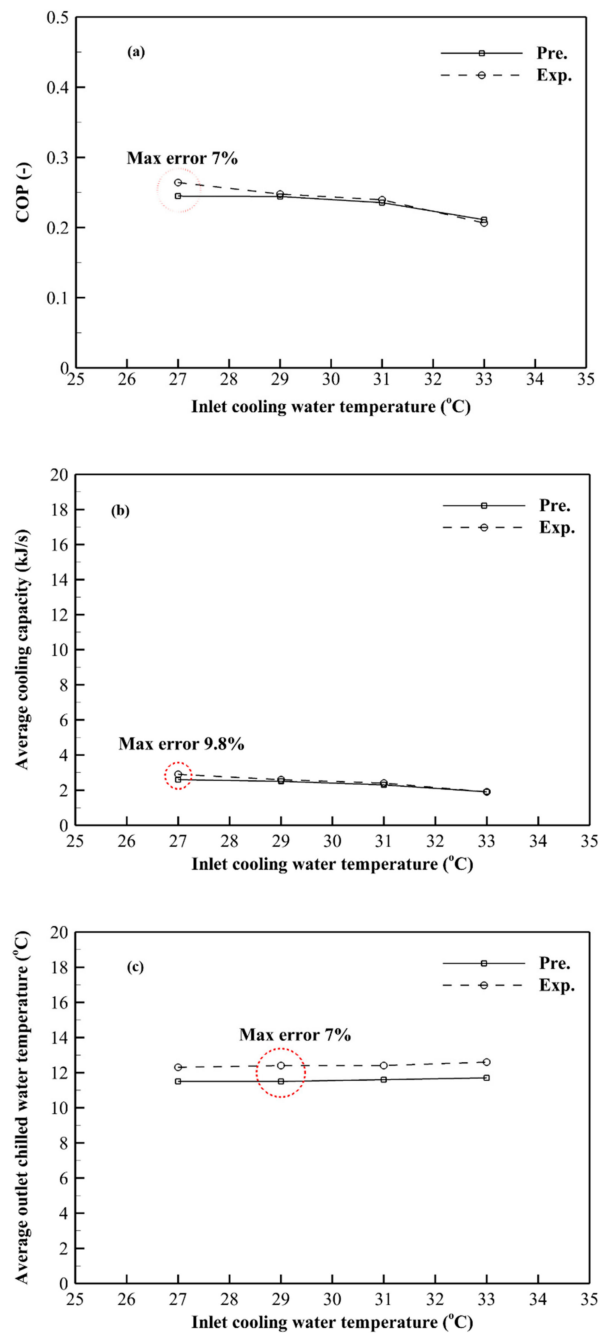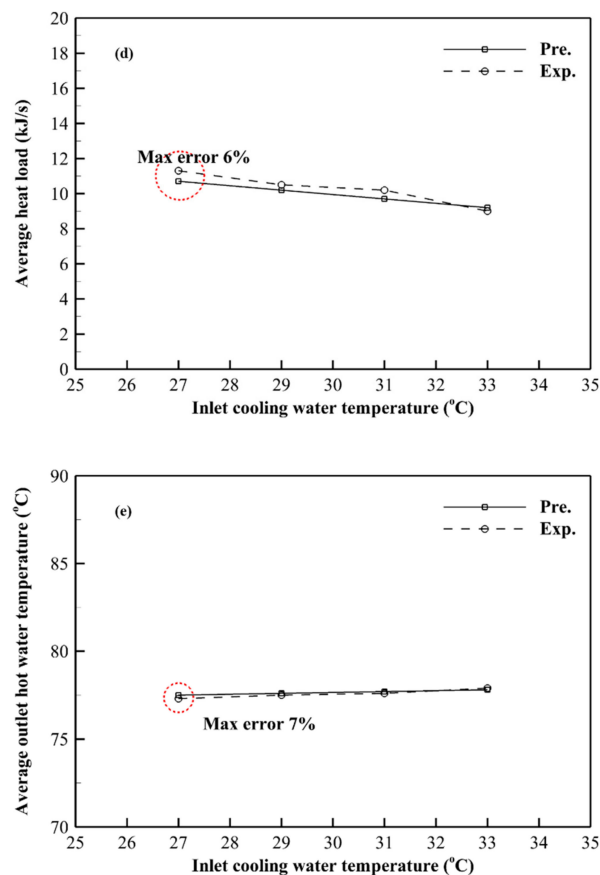

Figure 5. *Cont.*

Figure 5. Comparison study between experimental results and predicted results: (**a**) coefficient of performance (COP); (**b**) cooling capacity; (**c**) average outlet chilled water temperature; (**d**) average heat load; and (**e**) average outlet hot water temperature.

3.2. Influence of Inlet Hot-Water Temperature on the System Performance

To investigate the influence of the inlet hot-water temperature on the two-bed AD system, numerical analysis was conducted with various inlet hot-water temperatures ranging from 60 °C to 80 °C under the operating conditions given in Table 2. Figure 6a,b present the cooling capacity and the COP, respectively, according to the inlet hot water temperature. When the silica-gel is employed as an adsorbent, the cooling capacity of two-bed type AD system increases linearly from 2.60 to 7.88 kW with an increase in the inlet hot-water temperature from 60 to 80 °C. The COP also increases linearly from 0.26 to 0.44 with the increase in the inlet hot water temperature. This is because the silica-gel has a linear shape isotherm graph according to the pressure.

When the aluminum fumarate is employed as an adsorbent, the cooling capacity asymptotically increases from 4.24 to 5.60 kW. The COP increases from 0.41 to 0.45 with an increase in the inlet hot-water temperature from 60 to 64 °C. However, when the inlet hot-water temperature is higher than 64 °C, the COP decreases dramatically from 0.45 to 0.36 with an increase in the inlet hot water temperature. Although the cooling capacity and COP are not higher than those obtained with the silica-gel adsorbent at the highest inlet hot-water temperature, they are higher at the lower inlet hot water temperature. That clearly shows the advantage of aluminum fumarate as an adsorbent which has an S-shape isotherm at low inlet hot water temperature; however, the issue of low cooling capacity remains a challenge.
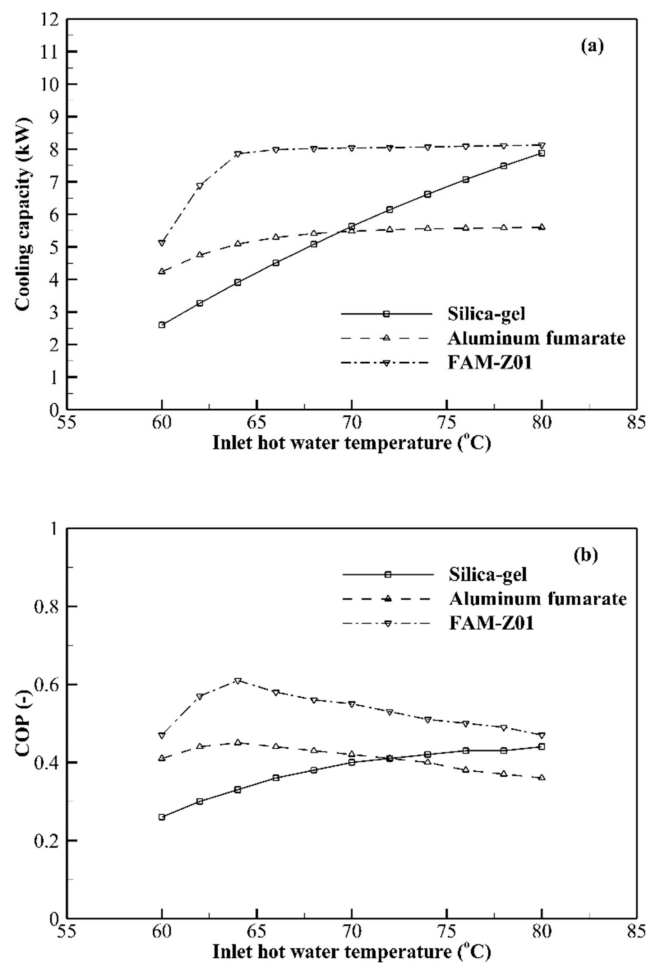
Figure 6. Influence of inlet hot-water temperature on: (**a**) cooling capacity and (**b**) COP.

When the FAM-Z01 is employed as an adsorbent, the cooling capacity asymptotically increases from 5.13 to 8.13 kW. The COP also shows the peak point as 0.61 at the inlet hot-water temperature of 64 °C. The trend of increase of cooling capacity and COP with FAM-Z01 is similar to that of the aluminum fumarate due to its S-shape isotherm graph.

However, the cooling capacity and COP is around 1.5 times larger than those of silica-gel. This is because the adsorption/desorption rate of aluminum fumarate is higher around two times that of FAM-Z01, but the pre-exponential constant of surface diffusivity of aluminum fumarate is far lower than that of FAM-Z01. That clearly shows that the physical properties of adsorbent and the adsorption and desorption rate of adsorbent can simultaneously affect the system performance.

Consequently, although the silica-gel system can have a higher cooling capacity than aluminum fumarate at the high inlet hot-water temperature, it can lead to low COP and high thermal energy consumption. Meanwhile, the cooling capacity for aluminum fumarate is lower than that of silica-gel; however, it can achieve the same COP at a lower inlet hot-water temperature. The potential value of the adsorption and desorption rate for aluminum fumarate was almost double that of FAM-Z01. However, the cooling capacity and COP of FAM-Z01 were higher than those of the aluminum fumarate. This is because the physical properties of the FAM-Z01 such as the low pre-exponential constant of surface diffusivity and higher heat of adsorption are better than those of aluminum fumarate. In addition, the system performance with FAM-Z01 is higher than that with silica-gel at all given inlet hot water temperature.

3.3. Influence of Cooling Water Temperature on the System Performance

To investigate the influence of the cooling water temperature on the system performance, the performance evaluation of the two-bed type AD system was conducted under the given operating conditions and fixed inlet hot-water temperature of 60 °C. Figure 7a,b present the cooling capacity and the COP, respectively, with respect to the inlet cooling water temperature.
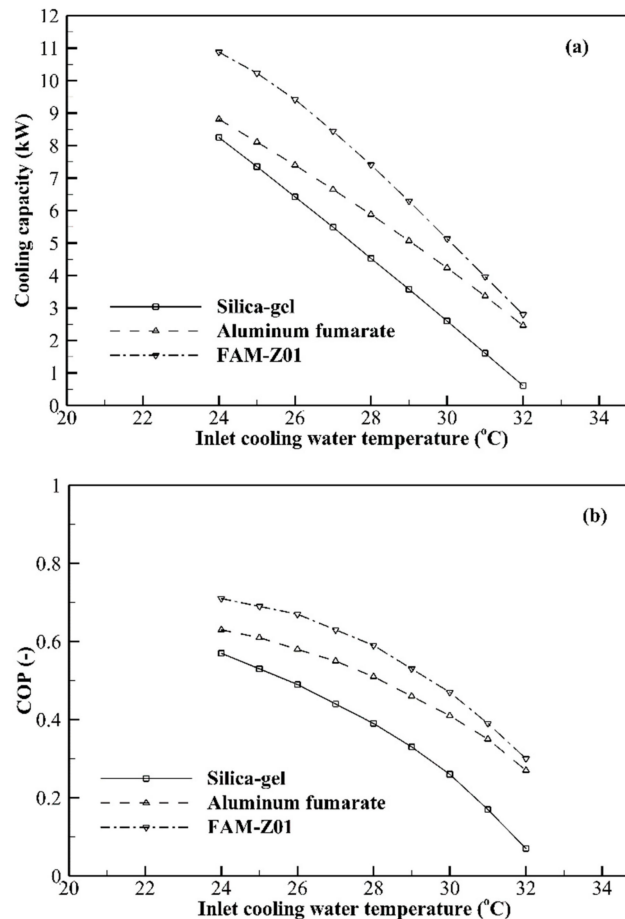

Figure 7. Influence of inlet cooling water temperature on: (**a**) cooling capacity and (**b**) COP.

The inlet hot-water temperature of 60 °C is assumed to be plausibly obtained from the low quality waste heat. When the silica-gel is employed on the two-bed AD system as an adsorbent, the cooling capacity and COP decrease dramatically from 8.25 to 0.62 kW and from 0.57 to 0.07, respectively, with an increase in the inlet cooling water temperature. As the aluminum fumarate is used as an adsorbent in the two-bed type AD system, the cooling capacity and COP also decrease from 8.81 to 2.46 kW and from 0.63 to 0.27, respectively, with an increase in the inlet cooling water temperature. When FAM-Z01 is used, the cooling capacity and COP show a similar trend of steep decrease like the aluminum fumarate according to the increase in the inlet cooling water temperature. The cooling capacity and COP decrease from 10.88 to 2.80 kW and from 0.71 to 0.30, respectively. When the FAM-Z01 was employed as an adsorbent, the decrease in COP was the steepest with the increase in the inlet cooling water temperature; this is because the decrease in the desorption rate with the increase inlet cooling water temperature is more sensitive than others. This work indicated that the increase of inlet cooling water temperature adversely affects the system performance for all the three adsorbents. An increase of inlet cooling water temperature can cause the degradation of system performance during the adsorption, and it also shows the disadvantage of an adsorbent which has an S-shape isotherm graph when the inlet cooling water temperature increases.

3.4. Influence of Chilled Water Temperature on the System Performance

The chilled water temperature directly affects the cooling capacity and COP of the AD system. A low inlet chilled-water temperature can restrain the evaporation and also decrease the system performance. Therefore, in this section, the influence of the inlet chilled-water temperature on the system performance was discussed under the given operating conditions. Figure 8a,b show the influence of inlet chilled water temperature on cooling capacity and COP at the inlet chilled water temperature range from 10 to 14 °C.
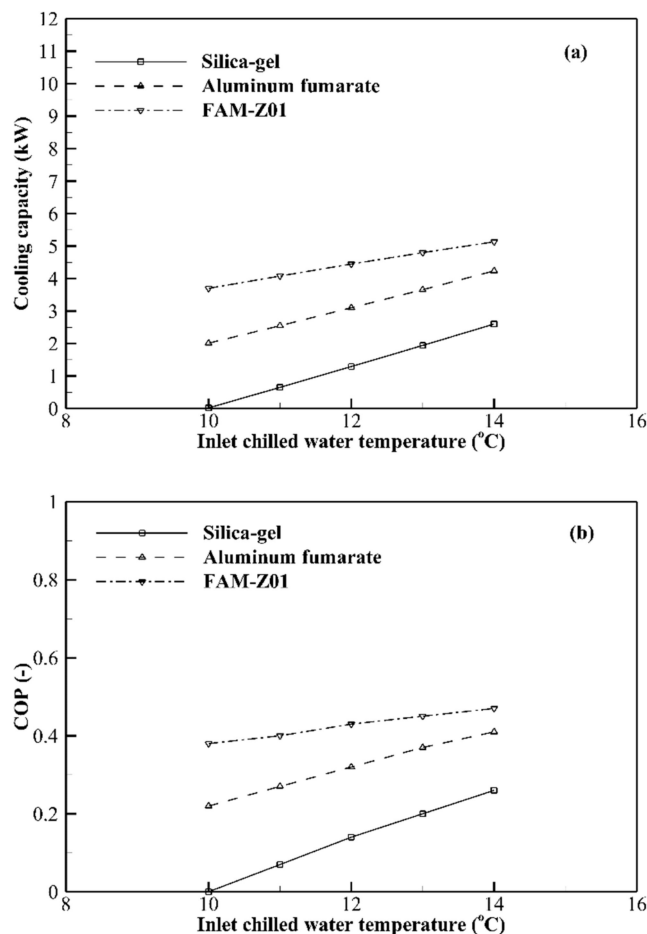

Figure 8. Influence of inlet chilled water temperature on: (**a**) cooling capacity and (**b**) COP.

When silica-gel was employed as an adsorbent, the cooling capacity increased from 0.02 to 2.60 kW with an increase in the inlet chilled water temperature from 10 to 14 °C, while the COP increased from 0 to 0.26. The system performance of the two-bed type AD system with aluminum fumarate adsorbent also increases with an increase in the inlet chilled-water temperature. The cooling capacity and COP increase from 2.01 to 4.24 kW and 0.22 to 0.41, respectively. In the case of the FAM-Z01, the cooling capacity and COP increase from 3.70 to 5.13 kW and 0.38 to 0.47 with an increase in the inlet chilled-water temperature.

We confirmed that low inlet chilled-water temperature leads to low system performance. Although the aluminum fumarate and FAM-Z01-based two-bed type AD system shows relatively better system performance than silica-gel-based systems, owing to the S-shape isotherm graph of the aluminum fumarate and FAM-Z01, the use of adsorbents which have S-shaped isotherm graphs could not mitigate the degradation of system performance from the decrease in the inlet chilled water temperature.

4. Discussion

In this study, we analyzed numerically, the influences of adsorbent types such as silica-gel, aluminum fumarate, and FAM-Z01 on the system performance for a two-bed type AD system under given operating conditions. Moreover, the influences of the physical properties and the shapes of isotherm graphs on the system performance were discussed with comparison studies with various adsorbents. Among the three different adsorbents, FAM-Z01 showed the best performance regarding the cooling capacity and COP. Although FAM-Z01 shows lower adsorption and desorption rates compared to aluminum fumarate, the physical properties of FAM-Z01 are better than aluminum fumarate. The FAM-Z01-based two-bed type AD system shows a maximum cooling capacity of 5.13 kW and COP of 0.47. In addition, the system performance of AD with FAM-Z01 shows better performance than that with silica-gel and aluminum fumarate at all inlet hot water temperature ranges including 60 °C. It means that the AD system with FAM-Z01 has great potential to be operated with waste heat and sustainable energy sources, such as solar and geothermal energies. The adsorbents which have S-shape isotherm graphs showed better system performances regarding the cooling capacity and COP than the adsorbent which had a linear-shape isotherm graph. The comparison study between aluminum fumarate and FAM-Z01 was conducted to evaluate the influences of the physical properties and adsorption and desorption rates on the system performance. In addition, through this study, we revealed that both physical properties and adsorption and desorption rates simultaneously, can affect the system performance. In summary, to enhance the system performance, the adsorbent for AD system should have a high pre-exponential constant of surface diffusivity and low activation energy of diffusion, low particle size, low specific heat, and low heat of adsorption.

Author Contributions: J.-G.L. carried out the development of the concept of the paper, performed the literature study, planned the paper and objectives, did the simulation study, analyzed the data, and wrote the paper. K.J.B. helped to search the literature and organize the data. O.K.K. supervised and advised this work. All authors have read and agreed to the published version of the manuscript.

Conflicts of Interest: The authors declare no conflict of interest.

Nomenclature

A_0	Isotherm coefficient (-)
B	Isotherm coefficient (-)
A	Area (m^2)
C_P	Specific heat (J/kgK)
D_{SO}	Pre-exponential constant of surface diffusivity (m^2/s)
E_a	Activation energy of surface diffusion (J/mol)
K	Isotherm coefficient (-)
K_{Henry}	Isotherm coefficient (-)
K_{Sips}	Isotherm coefficient (-)
k_{sap}	Overall mass transfer coefficient (W/m^{2}K)
L_w	Latent heat of vaporization (J/kg)
$\dot{m}$	Mass flow rate (kg/s)
n	Isotherm coefficient (-)
P	Pressure (Pa)
q	Adsorption rate (g/g)
Q_{st}	Heat of adsorption (kJ/kg)
Q	Heat (kW)

R	Ideal gas constant (J/kgK)
r_p	Particle size (m)
T	Temperature (K)
t	Time (s)
U	overall heat transfer coefficient (W/m^{2}K)
W	Weight (kg)
$W_{F,HX}$	Weight of fin (kg)
$W_{K,HX}$	Weight of heat transfer tube (kg)
Symbol	
β	Isotherm coefficient (-)
Superscripts	
*	*Equilibrium*
max	*Maximum*
Subscripts	
Al	*Aluminum*
Cu	*Cupper*
Chilled	Chilled water
Cond	Condenser
CW	Cooling water
EW	Refrigerant in evaporator
Eva	Evaporator
HX	Heat exchanger
HW	Hot water
S	Saturation
W	Water

References

1. Al-Mousawi, F.N.; Al-Dadah, R.; Mahmoud, S. Novel Adsorption System for Cooling and Power Generation Utilizing Low Grade Heat Sources. In Proceedings of the 2016 International Conference for Students on Applied Engineering (ICSAE), Newcastle upon Tyne, UK, 20–21 October 2016; pp. 334–339.
2. Saha, B.B.; Boelman, E.C.; Kashiwagi, T. Computer simulation of a silica gel-water adsorption refrigeration cycle-the influence of operating conditions on cooling output and COP. *Unkn. J.* **1995**, *101*, 348–357.
3. Rezk, A.R.; Al-Dadah, R.K. Physical and operating conditions effects on silica gel/water adsorption chiller performance. *Appl. Energy* **2012**, *89*, 142–149. [CrossRef]
4. Wang, D.; Xia, Z.; Wu, J.; Wang, R.; Zhai, H.; Dou, W. Study of a novel silica gel–water adsorption chiller. Part, I. Design and performance prediction. *Int. J. Refrig.* **2005**, *28*, 1073–1083. [CrossRef]
5. Wang, D.; Wu, J.; Xia, Z.; Zhai, H.; Wang, R.; Dou, W. Study of a novel silica gel–water adsorption chiller. Part II. Experimental study. *Int. J. Refrig.* **2005**, *28*, 1084–1091. [CrossRef]
6. Chen, C.; Wang, R.; Xia, Z.; Kiplagat, J.; Lu, Z. Study on a compact silica gel-water adsorption chiller without vacuum valves: Design and experimental study. *Appl. Energy* **2010**, *87*, 2673–2681. [CrossRef]
7. Alahmer, A.; Wang, X.; Al-Rbaihat, R.; Alam, K.A.; Saha, B.B. Performance evaluation of a solar adsorption chiller under different climatic conditions. *Appl. Energy* **2016**, *175*, 293–304. [CrossRef]
8. Chua, H.; Ng, K.; Wang, W.; Yap, C.; Wang, X. Transient modeling of a two-bed silica gel-water adsorption chiller. *Int. J. Heat Mass Transf.* **2004**, *47*, 659–669. [CrossRef]
9. Li, S.; Wu, J. Theoretical research of a silica gel-water adsorption chiller in a micro combined cooling, heating and power (CCHP) system. *Appl. Energy* **2009**, *86*, 958–967. [CrossRef]
10. Ng, K.; Chua, H.; Chung, C.; Loke, C.; Kashiwagi, T.; Akisawa, A.; Saha, B.B. Experimental investigation of the silica gel-water adsorption isotherm characteristics. *Appl. Therm. Eng.* **2001**, *21*, 1631–1642. [CrossRef]
11. Chang, W.-S.; Wang, C.-C.; Shieh, C.-C. Design and performance of a solar-powered heating and cooling system using silica gel/water adsorption chiller. *Appl. Therm. Eng.* **2009**, *29*, 2100–2105. [CrossRef]
12. Freni, A.; Sapienza, A.; Glaznev, I.S.; Aristov, Y.I.; Restuccia, G. Experimental testing of a lab-scale adsorption chiller using a novel selective water sorbent "silica modified by calcium nitrate". *Int. J. Refrig.* **2012**, *35*, 518–524. [CrossRef]

13. Zhang, G.; Wang, D.; Zhang, J.; Han, Y.; Sun, W. Simulation of operating characteristics of the silica gel-water adsorption chiller powered by solar energy. *Sol. Energy* **2011**, *85*, 1469–1478. [CrossRef]

14. Rezk, A.; Al-Dadah, R.; Mahmoud, S.; Elsayed, A. Effects of contact resistance and metal additives in finned-tube adsorbent beds on the performance of silica gel/water adsorption chiller. *Appl. Therm. Eng.* **2013**, *53*, 278–284. [CrossRef]

15. Myat, A.; Choon, N.K.; Thu, K.; Kim, Y.-D. Experimental investigation on the optimal performance of Zeolite-water adsorption chiller. *Appl. Energy* **2013**, *102*, 582–590. [CrossRef]

16. Li, A.; Ismail, A.B.; Thu, K.; Ng, K.C.; Loh, W.S. Performance evaluation of a zeolite-water adsorption chiller with entropy analysis of thermodynamic insight. *Appl. Energy* **2014**, *130*, 702–711. [CrossRef]

17. Hong, S.W.; Ahn, S.H.; Chung, J.D.; Bae, K.J.; Cha, D.A.; Kwon, O.K. Characteristics of FAM-Z01 compared to silica gels in the performance of an adsorption bed. *Appl. Therm. Eng.* **2016**, *104*, 24–33. [CrossRef]

18. Kim, Y.-D.; Thu, K.; Ng, K.C. Adsorption characteristics of water vapor on ferroaluminophosphate for desalination cycle. *Desalination* **2014**, *344*, 350–356. [CrossRef]

19. Rezk, A.; Al-Dadah, R.; Mahmoud, S.; Elsayed, A. Characterisation of metal organic frameworks for adsorption cooling. *Int. J Heat Mass Transf.* **2012**, *55*, 7366–7374. [CrossRef]

20. Rezk, A.; Raya, A.-D.; Mahmoud, S.; Elsayed, A. Investigation of Ethanol/metal organic frameworks for low temperature adsorption cooling applications. *Appl. Energy* **2013**, *112*, 1025–1031. [CrossRef]

21. Solovyeva, M.; Gordeeva, L.; Krieger, T.; Aristov, Y.I. MOF-801 as a promising material for adsorption cooling: Equilibrium and dynamics of water adsorption. *Energy Convers. Manag.* **2018**, *174*, 356–363. [CrossRef]

22. Teo, H.W.B.; Chakraborty, A.; Kitagawa, Y.; Kayal, S. Experimental study of isotherms and kinetics for adsorption of water on Aluminium Fumarate. *Int. J. Heat Mass Transf.* **2017**, *114*, 621–627. [CrossRef]

23. Teo, H.W.B.; Chakraborty, A.; Kayal, S. Formic acid modulated (fam) aluminium fumarate MOF for improved isotherms and kinetics with water adsorption: Cooling/heat pump applications. *Microporous Mesoporous Mater.* **2018**, *272*, 109–116. [CrossRef]

24. Youssef, P.G.; Dakkama, H.; Mahmoud, S.M.; AL-Dadah, R.K. Experimental investigation of adsorption water desalination/cooling system using CPO-27Ni MOF. *Desalination* **2017**, *404*, 192–199. [CrossRef]

25. Al-Mousawi, F.N.; Al-Dadah, R.; Mahmoud, S. Low grade heat driven adsorption system for cooling and power generation using advanced adsorbent materials. *Energy Convers. Manag.* **2016**, *126*, 373–384. [CrossRef]

26. Han, B.; Chakraborty, A. Water adsorption studies on synthesized alkali-ions doped Al-fumarate MOFs and Al-fumarate+ zeolite composites for higher water uptakes and faster kinetics. *Microporous Mesoporous Mater.* **2019**, *288*, 109590. [CrossRef]

27. Youssef, P.; Mahmoud, S.; Al-Dadah, R.; Elsayed, E.; El-Samni, O. Numerical Investigation of Aluminum Fumarate MOF adsorbent material for adsorption desalination/cooling application. *Energy Procedia* **2017**, *142*, 1693–1698. [CrossRef]

28. Elsayed, E.; Raya, A.-D.; Mahmoud, S.; Elsayed, A.; Anderson, P.A. Aluminium fumarate and CPO-27 (Ni) MOFs: Characterization and thermodynamic analysis for adsorption heat pump applications. *Appl. Therm. Eng.* **2016**, *99*, 802–812. [CrossRef]